Materials Research Proceedings **26** (2023) 331-336 https://doi.org/10.21741/9781644902431-54

Impacts analysis in the rocking of masonry circular arches

Paolo Bisegna[a], Simona Coccia[b], Mario Como[c], Nicola Nodargi[d]

University of Rome "Tor Vergata", Italy

[a]bisegna@uniroma2.it, [b]coccia@ing.uniroma2.it, [c]como@uniroma2.it, [d]nodargi@ing.uniroma2.it

Keywords: Masonry, Circular Arch, No Tension Material, Rocking, Restitution Coefficient

Abstract. The in-plane rocking of a masonry arch is studied. The starting motion of the arch is assumed to take place along the four-link failure mechanism ***u*** corresponding to a constant distribution of horizontal loads proportional to the arch self-weight. During such a motion, if overturning does not occur, the arch returns to the undeformed configuration, with all the hinges of the mechanism ***u*** simultaneously closing. At such an instant, impacts occur, implying a motion exchange and a subsequent movement of the arch along a new four-link mechanism ***u'***. A novel impact model, different from the one available in literature, is here proposed. The restitution coefficient is computed by applying the linear and angular momentum impulse theorems. The rocking mechanism ***u'*** of the arch after the impact is determined under the condition of minimum energy expense at the impact.

Introduction

Fig. 1 shows a free-standing stone column over a supporting plane that, hit by a horizontal impulse from left to right, puts itself in a rocking motion. The friction between the column and its supporting plane is sufficiently high, and the column is sufficiently slender, to avoid occurrence of sliding or bouncing during the motion. The column thus rotates around the point O of its basis up to the attainment of a maximum rotation angle; then, if overturning does not occur, it inverts its motion until an impact occurs at the opposite point O' of its base. Afterwards, the column continues to rotate with non-harmonic oscillations of reduced amplitudes and periods until it stops. This type of motion is called "rocking".

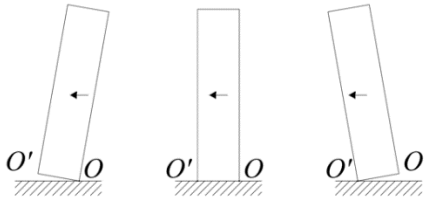

Figure 1. Rocking motion of a free-standing masonry wall

A fundamental paper by Housner [1], concerning the study of the behaviour of a free-standing stone column placed upon a rigid horizontal base and undergoing rocking motion, set the basis for the application of these concepts in the assessment of the dynamical behaviour of masonry constructions. The first description of the in-plane motion of a masonry circular arch, without any impact analysis, can be found in [2]. More recently, energy dissipation models of the impacts occurring in the rocking of the arch, considered as a rigid body four-link mechanism, have been given in [3, 4, 5]. In spite of the numerous researches on the subject, the definition of the mechanical model of the impacts in the rocking motion of the masonry arch is still debated and a new model is here proposed.

Materials Research Proceedings **26** (2023) 331-336 https://doi.org/10.21741/9781644902431-54

The rocking mechanism of the arch

A horizontal ground acceleration pulse, acting from right to left, is assumed to hit a masonry arch. If the magnitude of the acceleration pulse exceeds the incipient rocking value A_L, the arch starts to move along a four-link mechanism ***u***. Both the incipient rocking acceleration A_L and the mechanism ***u*** can be straightforwardly computed by the Limit Analysis theorems [6]. During such a motion, if overturning does not occur, the arch, moving from right to left, returns to the undeformed configuration, with all the hinges of the mechanism ***u*** simultaneously closing. At that instant, a motion exchange takes place and a new motion, still from right to left, develops along a new four-link mechanism ***u'***.

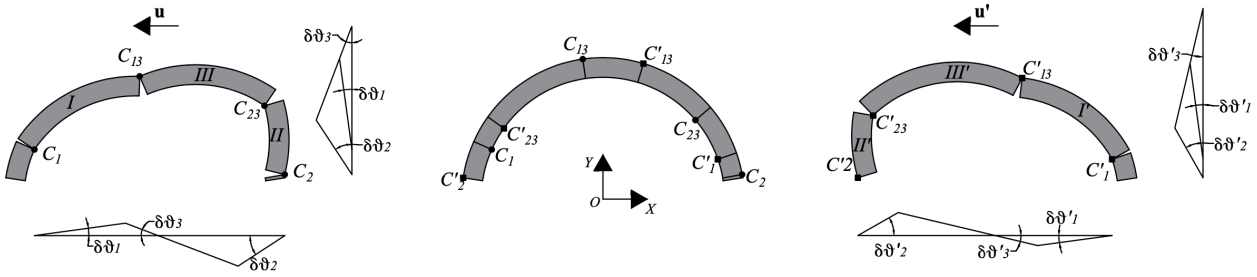

*Figure 2. Hinge locations in mechanisms **u** and **u'***

In the mechanism ***u*** the rotations $\delta\theta_2$ and $\delta\theta_3$ can be expressed as a function of $\delta\theta_1$ as:

$$\delta\theta_3 = k_{31}\delta\theta_1; \quad \delta\theta_2 = k_{21}\delta\theta_1 \tag{1}$$

where the coefficients k_{i1} are evaluated in the undeformed configuration as function of the coordinates of the centres of the rotation:

$$k_{31} = \frac{x_{C_{13}} - x_{C_1}}{x_{C_3} - x_{C_{13}}}; \quad k_{21} = k_{31}\frac{x_{C_{23}} - x_{C_3}}{x_{C_2} - x_{C_{23}}} \tag{2}$$

Analogous expressions hold for the mechanism ***u'***.

A new impact model

An essential problem to be addressed for computing the mechanism ***u'*** after the impact is the localization of the internal impulsive forces arising at the instant when impacts occur. A first step in solving that problem requires to recognize that the locations of the hinges of ***u'*** are impact points, thus transmitting impulsive internal forces.

Some researchers, basing on the analogy with the behaviour of Housner's column, account for impacts occurring at the opposite side of the sections containing the hinges of the mechanism ***u***, which are *closing* [2, 3]. However, besides those unquestionable impact points, also the locations of the hinges of ***u'***, i.e. the points around which the arch segments pivot in the new motion of the arch after the impact, should be recognized as impact points.

In fact, consider the instant when the hinges of the mechanism ***u*** begin to close while the new mechanism ***u'*** is taking place. If the hinges of ***u'*** develop at the same sections of the arch where the hinges of former mechanism ***u*** are located (Fig. 3), the passage from ***u*** to ***u'*** is similar to what happens in the Housner column (Fig. 1) and it is recognized that impacts occur at points where the hinges of the new mechanism are located.

Consider then the case in which the hinges of ***u'*** develop at sections different from those of the former mechanism ***u***. While the hinges of ***u*** are closing, inertial effects force the arch to develop the new mechanism ***u'***. Impulsive compressive forces flow across the closed sections of ***u*** while the sections including the new hinges of ***u'*** begin to open and start to reciprocally rotate, thus

Materials Research Proceedings **26** (2023) 331-336 https://doi.org/10.21741/9781644902431-54

impacting one against the other. So, an impact occurs at the points where the hinges of the mechanism ***u'*** are located and therein compressive impulse forces are transmitted (Fig. 4).

The impulsive forces can be determined by using the linear and angular momentum impulse theorems, as shown below.

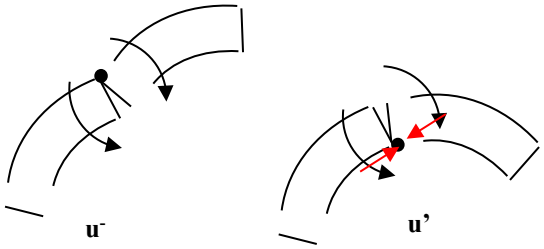

4

*Figure 3. The case, similar to the Housner column, in which the hinges of **u'** occur at the same sections where the hinges of **u** are located*

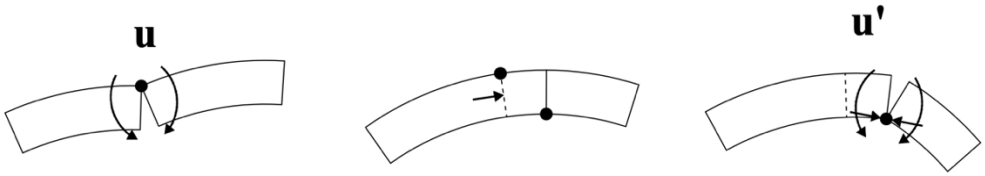

*Figure 4. The case in which hinges of **u'** develop at sections different from those of the former mechanism **u***

However, the issue to define the locations of the hinges of the mechanism ***u'*** developing in the arch after the impact remains to be solved. Here it is postulated that those hinges are formed at locations producing the minimum energy expense at the impacts, i.e. maximizing the restitution coefficient *r*.

In passing, some authors in the literature assume that the locations of the hinges of the mechanism ***u'*** are at the mirrored locations of the hinges of the mechanism ***u***. However, that assumption does not generally imply the minimum energy expense at the impact.

To that purpose, it is recalled that *I, II, III* denote the arch segments included between the sections through the hinges C_1, C_{13}, C_{23}, C_2 of the mechanism ***u***, whereas *I', II', III'* denote the arch segments included between the sections through the hinges C_1', C_{13}', C_{23}', C_2' of the mechanism ***u'*** (Fig. 2). If considered altogether, the sections through the hinges of the mechanisms ***u*** and ***u'*** pinpoint seven bodies, labelled as 1, …, 7, such that the arch segments of those mechanisms can be recovered as (Fig. 5):

$$\begin{array}{lll} I = 2 \cup 3 & II = 6 \cup 7 & III = 4 \cup 5 \\ I' = 5 \cup 6 & II' = 1 \cup 2 & III' = 3 \cup 4 \end{array} \qquad (3)$$

Let m_i and $I_{O,i}$ respectively denote the mass and the polar moment of inertia around the centre *O* of the *i*th of those bodies. It is noticed that the kinematics of that body before [resp., after] the impact is completely described by its angular velocity $\dot{\theta}_i \mathbf{k}$ [resp., $\dot{\theta}_i' \mathbf{k}$], with **k** as a unit vector orthogonal to the plane of the arch, and by its absolute centre of rotation C_i [resp., C_i'].

Materials Research Proceedings **26** (2023) 331-336 https://doi.org/10.21741/9781644902431-54

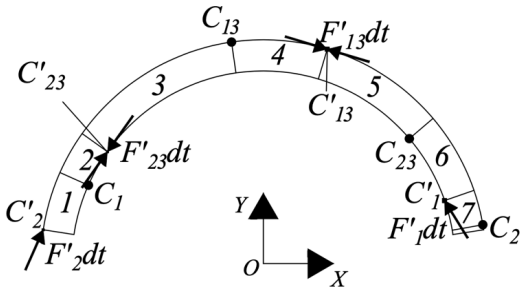

*Figure 5. The seven bodies composing the mechanisms **u** and **u'***

Indeed, due to the compatibility conditions of the mechanism $\boldsymbol{u}$ [resp., $\boldsymbol{u'}$], the angular velocities can be expressed in terms of a single free parameter $\dot{q}$ [resp., $\dot{q}'$] by:

$$\dot{\theta}_i = \Theta_i \dot{q}; \quad \dot{\theta}'_i = \Theta'_i \dot{q}' \tag{4}$$

where Θ_i [resp., Θ'_i] are known geometrical coefficients (e.g., if the choice $\dot{q} = \dot{\theta}_1$ [resp., $\dot{q}' = \dot{\theta}'_1$] is made, it follows that $\Theta_1 = 1$, $\Theta_2 = k_{21}$ and $\Theta_3 = k_{31}$ [resp., $\Theta'_1 = 1$, $\Theta'_2 = k'_{21}$ and $\Theta'_3 = k'_{31}$], consistently with Equation (1)).

Accordingly, the linear momentum $\boldsymbol{p}_i$ [resp., $\boldsymbol{p}'_i$] and the angular momentum $\boldsymbol{L}_{O,i}$ [resp., $\boldsymbol{L}'_{O,i}$] around the pole O of the ith body before [resp., after] the impact are given by (equations to be read without [resp., with] apex):

$$\boldsymbol{p}_i = m_i \boldsymbol{V}_{Gi} = [m_i \boldsymbol{k} \times (G_i - C_i)]\Theta_i \dot{q} \tag{5}$$

$$\boldsymbol{L}_{O,i} = I_{G_i,i}\dot{\theta}_i \mathbf{k} + (G_i - O) \times \boldsymbol{p}_i = \left[I_{G_i,i} + m_i (G_i - O) \cdot (G_i - C_i)\right]\Theta_i \dot{q} \boldsymbol{k} \tag{6}$$

where $\boldsymbol{V}_{Gi}$ denotes the velocity of the centre of gravity G_i of the ith body.

As the impact is of very short duration, very large impulsive forces act on the arch, producing finite changes of velocity of its various parts without significant changes in configuration. Accordingly, during the impact, all ordinary forces (such as gravity) are negligible, and no change of configuration of the arch needs to be considered.

On such a basis, the computation of the unknown parameter $\dot{q}'$ can be achieved by including among the unknowns the impulsive forces $\boldsymbol{F}'_1 dt$ and $\boldsymbol{F}'_2 dt$ carried out by the hinges C'_1 and C'_2 at the impact, and by formulating a system of five equations in five unknowns.

In detail, those equations are:

- the linear momentum impulse theorem for the portion of the arch between C'_1 and C'_2 along x and y directions (Fig. 6):

$$\sum_{i=1}^{6} \boldsymbol{p}_i + (\boldsymbol{F}'_1 + \boldsymbol{F}'_2)dt = \sum_{i=1}^{6} \boldsymbol{p}'_i \tag{7}$$

- the angular momentum impulse theorem for the portion of the arch between C'_1 and C'_2 about the center O (Fig. 6):

$$\sum_{i=1}^{6} \boldsymbol{L}_{O,i} + (C'_1 - O) \times \boldsymbol{F}'_1 dt + (C'_2 - O) \times \boldsymbol{F}'_2 dt = \sum_{i=1}^{6} \boldsymbol{L}'_{O,i} \tag{8}$$

- the angular momentum impulse theorem for the portion of the arch between C'_{13} and C'_1 about the point C'_{13} (Fig. 7):

$$\sum_{i=5}^{6} \boldsymbol{L}_{C'_{13},i} + (C'_1 - C'_{13}) \times \boldsymbol{F}'_1 dt = \sum_{i=5}^{6} \boldsymbol{L}'_{C'_{13},i} \tag{9}$$

Materials Research Proceedings **26** (2023) 331-336 https://doi.org/10.21741/9781644902431-54

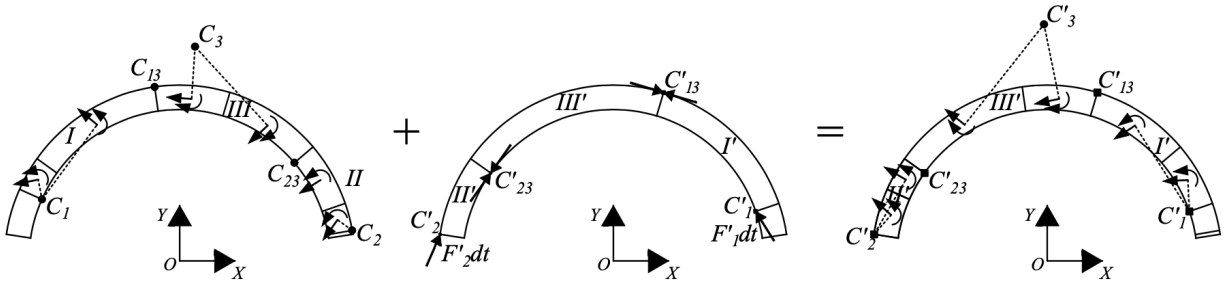

Figure 6. Linear and angular momentum impulse theorems during the impact

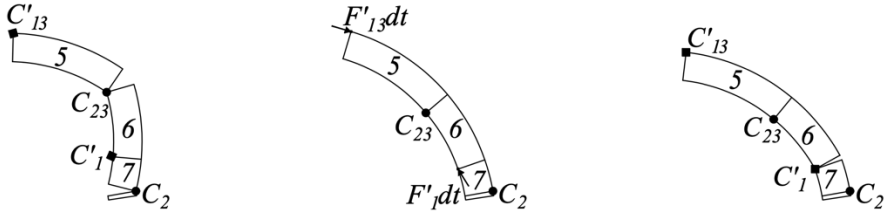

Figure 7. Angular momentum impulse theorem around the point C'_{13}

- the angular momentum impulse theorem for the portion of the arch between C'_2 and C'_{23} about the point C'_{23} (Fig. 8):

$$\sum_{i=1}^{2} \boldsymbol{L}_{C'_{23},i} + (C'_2 - C'_{23}) \times \boldsymbol{F}'_2 dt = \sum_{i=1}^{2} \boldsymbol{L}'_{C'_{23},i} \qquad (10)$$

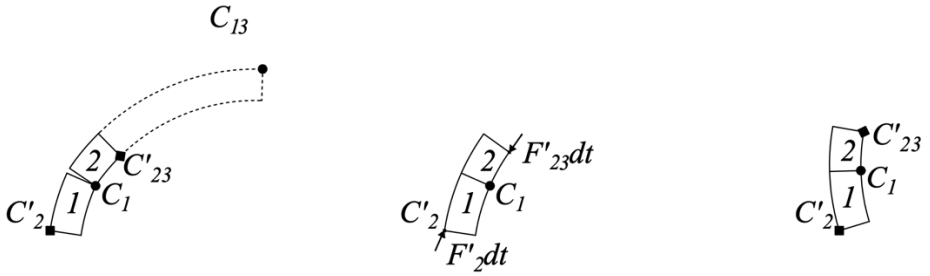

Figure 8. Angular momentum impulse theorem around the point C'_{23}

It is remarked that the angular momentum impulse theorem equations (9) and (10) are purposely written in such a way that the impulsive forces explicated by the internal hinges C'_{23} and C'_{13} are not explicitly involved (Fig. 5).

After solving Eqs. (7)–(10), and hence computing the free parameter $\dot{q}'$ of the arch mechanism ***u'***, the angular velocities $\dot{\theta}'_i$ follow from Eq. (4), whence it is a simple matter to compute the restitution coefficient of the arch as the ratio of the kinetic energy after the impact to the kinetic energy before the impact [1].

Furthermore, it is highlighted that *r* depends on the arch geometry and location of the hinges before the impact, which are known in advance, and by the location of the hinges after the impact, which are not. Hence, the latter are assumed as the unknowns of a nonlinear optimization problem, aimed at determining the maximum value of *r,* i.e. the minimum value of energy dissipation, among the various possible mechanisms ***u'***.

Numerical applications

A circular arch with an angle of embrace equal to 180°, a ratio t/R_m equal to 0.15 is considered for a numerical application of the proposed model. The mean radius R_m does not influence the results. The failure acceleration A_L results to be 0.1443. The mechanisms ***u*** before the impact, and the mechanism ***u'*** after the impact that maximize the restitution coefficient r, are shown in Fig. 10. It is remarked that the hinges of the mechanism ***u'*** are not in the mirrored location of the hinges of the mechanism ***u***. The corresponding maximum value of the restitution coefficient r results to be 0.6812.

Finally, the new concept of impulse line is introduced. Analogously to the thrust line, which graphically depicts the equilibrium between applied loads (including inertia forces) and constraint reactions at regular instants of motion, the impulse line depicts the equivalence between impulsive forces and variations of linear and angular momenta at impact instants. The impulse line at the impact instant relevant to the present case study is depicted in Fig. 10. It passes through the indrados and the extrados of the arch at sections where the hinges of ***u'*** take place. It can be shown that the impulse line is statically admissible, i.e. it is entirely contained within the thickness of the arch, if and only if the post-impact mechanism ***u'*** maximizes the restitution coefficient r over the space of kinematically admissible post-impact mechanisms.

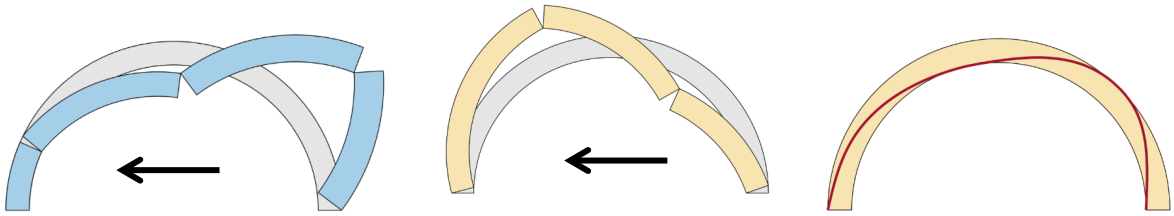

*Figure 10. Mechanisms **u** and **u'** and impulse line at the impact instant*

References

[1] G.W. Housner, The behaviour of inverted pendulum structures during earthquakes. Bulletin of the Seismological Society of America, 53(2), 403-417, 1963. https://doi.org/10.1785/BSSA0530020403

[2] I.J. Oppenheim, The masonry arch as a de mechanism under base motion. Earthquake Engineering and Structural Dynamics, 21, 1005-1017, 1992. https://doi.org/10.1002/eqe.4290211105

[3] L. De Lorenzis, M. DeJong, J. Ochsendorf, Failure of masonry arches under impulse base motion. Earthquake Engineering and Structural Dynamics, 36, 2119–2136, 2007. https://doi.org/10.1002/eqe.719

[4] M.J. DeJong, L. De Lorenzis, S. Adams, J.A. Ochsendorf, Rocking Stability of Masonry Arches in Seismic Regions. Earthquake Spectra, 24(4), 847–865, 2008. https://doi.org/10.1193/1.2985763

[5] L.P. Kollár, T. Ther, Numerical model and dynamic analysis of multi degree of freedom masonry arches, Earthquake Engineering & Structural Dynamics, 48(7), 709-730, 2019. https://doi.org/10.1002/eqe.3158

[6] M. Como, Statics of Historic masonry Constructions, 3rd ed., Springer, Heidelberg, 2017. https://doi.org/10.1007/978-3-319-54738-1